



ELSEVIER

Available online at www.sciencedirect.com

SCIENCE @ DIRECT®

Journal of Non-Crystalline Solids 315 (2003) 134–143

JOURNAL OF
NON-CRYSTALLINE SOLIDS

www.elsevier.com/locate/jnoncrysol

Optical properties of thermally evaporated amorphous $\text{As}_{40}\text{S}_{60-x}\text{Se}_x$ films

J.M. González-Leal^{a,*}, R. Prieto-Alcón^b, J.A. Angel^b, E. Márquez^b

^a Department of Chemistry, University of Cambridge, Lensfield Road, CB2 1EW Cambridge, UK

^b Departamento de Física de la Materia Condensada, Facultad de Ciencias, Universidad de Cádiz, 11.510 Puerto Real (Cádiz), Spain

Received 30 October 2001; received in revised form 5 February 2002

Abstract

Compositional dependencies of the optical properties of as-deposited amorphous $\text{As}_{40}\text{S}_{60-x}\text{Se}_x$ films ($x = 0, 20, 30, 40$ and 60 at.%), prepared by thermal evaporation, have been studied. The refractive index, n , and absorption coefficient, α , have been determined from the upper and lower envelopes of the transmission spectra, measured at normal incidence, in the spectral range from 400 to 2200 nm. An improved optical characterisation method for non-uniform films based on Swanepoel's ideas, which takes into account the weak absorption in the substrate, has been successfully employed, and it has allowed us to determine both the average thickness, \bar{d} , and the refractive index, n , of the films, with accuracies better than 1%. It has been found that the refractive index of the $\text{As}_{40}\text{S}_{60-x}\text{Se}_x$ samples increases with increasing x , over the entire spectral range, which is related to the increased polarizability, α_p , of the larger Se atoms, in comparison with S atoms. The values of the As effective coordination number, N_c , have been estimated from an analysis of the dispersion of the refractive index, and an increase in N_c with increasing Se content, from around 3.0 to 3.4, has been inferred.

© 2003 Elsevier Science B.V. All rights reserved.

PACS: 78.20.-e; 78.66.Jg; 78.20.Ci; 78.40.Fy

1. Introduction

Structural, optical and photoelectronic properties of chalcogenide amorphous semiconductors have been the subject of interest for about 40 years [1–4]. This interest has been stimulated both by basic scientific questions that have to be answered in order to understand the structure and properties

of these non-crystalline materials, and the need to assess their potential technological applications [4].

The present paper is concerned with the analysis of the optical properties of as-deposited amorphous $\text{As}_{40}\text{S}_{60-x}\text{Se}_x$ films ($x = 0, 20, 30, 40$ and 60 at.%), prepared by thermal evaporation. Although it is possible to find in the literature some papers dealing with both bulk [5–7] and thin films [8–12] within this particular composition line, to the best of our knowledge, there is no thorough study of its optical properties. Therefore, the lack of data in the literature concerning the optical characterisation of films of these particular materials, along

* Corresponding author. Tel.: +44-1223 336 532; fax: +44-1223 336 362.

E-mail addresses: jmg62@cam.ac.uk, juanmaria.gonzalez@uca.es (J.M. González-Leal).

with their attractive potential technological applications [10,11], highlight the significance of the present investigation.

2. Experimental

The $\text{As}_{40}\text{S}_{60-x}\text{Se}_x$ bulk glasses ($x = 0, 20, 30, 40$ and 60 at.%) were prepared according to the conventional melt-quenching method from 5 N purity elements. The synthesis was performed in evacuated quartz ampoules using a rocking furnace held at 700–750 °C for 8–24 h. Thin-film samples were prepared by vacuum evaporation of the powdered melt-quenched glassy material onto clean glass substrates (microscope slides). The thermal evaporation process was performed within a coating system at a pressure of about 10^{-3} Pa. During the deposition process the substrates were conveniently rotated by means of a planetary rotation system, which makes it possible to reduce the lack of uniformity in the thickness of the as-deposited glass films. The deposition rate was in the range 1–8 nm s^{-1} , measured continuously using the quartz microbalance technique. This deposition rate results in a film chemical composition which is very close to that of the starting bulk material. Chemical compositions of the chalcogenide films were found to be $\text{As}_{38.7\pm 0.8}\text{S}_{61.6\pm 0.7}$, $\text{As}_{39.8\pm 0.5}\text{S}_{39.9\pm 0.6}\text{Se}_{20.3\pm 0.3}$, $\text{As}_{38.9\pm 1.4}\text{S}_{31.0\pm 0.5}\text{Se}_{30.2\pm 1.7}$, $\text{As}_{39.1\pm 1.9}\text{S}_{22.2\pm 0.9}\text{Se}_{38.7\pm 1.9}$ and $\text{As}_{41.2\pm 1.8}\text{Se}_{58.8\pm 1.8}$, on the basis of electron microprobe X-ray analysis, using a scanning electron microscope. The lack of crystallinity in the films was systematically verified by X-ray diffraction measurements. The thicknesses of the amorphous $\text{As}_{40}\text{S}_{60-x}\text{Se}_x$ films studied were typically around 1 μm .

The optical transmission spectra were obtained, at normal incidence, by a double-beam ratio recording UV/Vis/NIR spectrophotometer with automatic computer-data acquisition, and the wavelength range analysed was between 400 and 2200 nm. A surface-profiling stylus was used to measure independently the film thicknesses, which were compared with those calculated from the transmission spectra. All optical measurements were performed at room temperature. Thin-film samples were kept in complete darkness until

measured to minimise exposure to light sources, which could lead to changes in the optical properties and possible oxidation of the films [13].

3. Theoretical considerations concerning the optical characterisation method

Optical characterisation methods based on the envelopes of the transmission spectrum assume the refractive index of the substrate, s , to be a known parameter, and its extinction coefficient, k_s to be equal to zero [14–17]. The refractive index is usually considered as a constant (typically 1.51 for silica) over the whole optical range, or it is independently derived from the transmission spectrum of the substrate, taken at normal incidence. We have checked, however, that the most popular glass substrates used by researchers (mainly borosilicate substrates) are weakly absorbing. Therefore, although the above approaches could be useful from a practical point of view, they are certainly not accurate nor valid for every kind of glass substrate and, in addition, over-estimated refractive-index values are often reported for the case of borosilicate substrates, when they are obtained from their transmission spectra. Hence, we suggest the use of both transmission, T_s , and reflection, R_s , spectra of the substrate, taken at normal incidence, in order to determine the refractive index, s , as well as the optical absorbance, $a_s (= \exp(-\alpha_s d_s))$, where α and d stand for the absorption coefficient and the thickness, respectively) of the substrate, by solving the following system of equations:

$$\begin{aligned} R_s(\lambda) - R_s(\lambda; s, a_s) &= 0, \\ T_s(\lambda) - T_s(\lambda; s, a_s) &= 0, \end{aligned} \quad (1)$$

where

$$R_s = \frac{R_1[1 + (1 - 2R_1)a_s^2]}{1 - R_1^2 a_s^2},$$

$$T_s = \frac{(1 - R_1)^2 a_s}{1 - R_1^2 a_s^2}$$

and

$$R_1 = \left| \frac{1 - s}{1 + s} \right|^2$$

is the Fresnel reflection factor for the air–substrate interface. We encourage, furthermore, the use of both s and a_s in the analytical equations involved in the calculation of the optical constants, refractive index, n , and extinction coefficient, k , as well as the thickness, d , of the film under study.

On the other hand, it is well known that thin films prepared by thermal evaporation usually show a significant lack of uniformity in thickness. Thus, keeping this idea, as well as the above comments on the absorption in glass substrates, in mind, we have obtained analytical equations for the upper and lower envelopes, T_+ and T_- , respectively, corresponding to a non-uniform thin dielectric film deposited onto a weakly absorbing substrate. In particular, we consider that the film thickness varies linearly over the film surface, within the interval $[\bar{d} - \Delta d, \bar{d} + \Delta d]$, although the formulation developed is also valid for some irregularities occurring periodically, in the form of surface roughness [16]. The wedging parameter Δd measures the actual variation in thickness at the extrema of the area illuminated by the spectrophotometer ($1 \times 4 \text{ mm}^2$).

Under the above-mentioned assumptions, the analytical expressions for the envelopes T_+ and T_- , are given as follows [18]:

$$T_{\pm}(\lambda; n, x, \Delta d, s, a_s) = \frac{1}{\theta} \frac{A}{(C^2 - D^2)^{1/2}} \tan^{-1} \left[\frac{C \pm D}{(C^2 - D^2)^{1/2}} \tan \theta \right], \quad (2)$$

where

$$A = (1 - R_1)(1 - R_2)(1 - R_3)aa_s,$$

$$C = 1 + R_2R_3a^2 - R_1R_2a^2a_s^2 + R_1R_2R_3a_s^2,$$

$$D = -2r_2r_3(1 - R_1a_s^2)a,$$

$$r_2 = \frac{1 - n}{1 + n}, \quad r_3 = \frac{n - s}{n + s},$$

$$R_2 = r_2^2, \quad R_3 = r_3^2,$$

$$\theta = 2\pi n \Delta d / \lambda,$$

$$a = \exp(-\alpha d)$$

and

$$\alpha = 4\pi k / \lambda.$$

The equations collected in (2) are the primary sources for the optical and geometrical characterisation of thin dielectric films with non-uniform thickness, deposited on weakly absorbing glass substrates. They can be expressed as a system of equations in the following implicit form:

$$\begin{aligned} T_+(\lambda) - T_+(\lambda; n, a, \Delta d) &= 0, \\ T_-(\lambda) - T_-(\lambda; n, a, \Delta d) &= 0. \end{aligned} \quad (3)$$

This system would need, obviously, one further equation in order to be solved. Thus, under the assumption of transparency, i.e., $a = 1$, which is valid for amorphous chalcogenides in the infrared spectral region [2–4], the system of equations can be solved for n and Δd , and a value for the wedging parameter can be determined by averaging the set of values of Δd obtained. However, it is important to note that due both to the fact that the assumption $a = 1$ is not valid at shorter wavelengths, and that the system is very sensitive to the errors made in the envelope drawing, specially at the largest wavelengths [16] (see Table 1), the corresponding values of Δd must not be included in the average. Once this geometrical parameter is known, the system of Eq. (3) can be solved for the refractive index, n , and the optical absorbance, a , for every wavelength, λ , from the spectral region of medium absorption to transparency. Nevertheless, a better approach is to limit the set of wavelength values considered in the calculations to those where the optical transmission spectrum and their envelopes are tangential, λ_{tan} [16]. This approach allows, using the equation for the interference fringes

$$2n\bar{d} = m\lambda_{\text{tan}}, \quad (4)$$

the accuracy of the results for the refractive index to be improved, as well as the average film thickness, \bar{d} , to be determined, following a well-known iterative procedure [15,16]. The order number, m , in Eq. (4), is an integer or a half-integer for an upper or a lower tangent point, respectively. All the details corresponding to this new approach for the optical and geometrical characterisation of thin dielectric films will be given elsewhere [18].

Table 1

Calculation of the average thickness of the film, \bar{d} , thickness variation, Δd , and refractive index, n , of a representative 1148 ± 5 nm thick amorphous $\text{As}_{40}\text{S}_{40}\text{Se}_{20}$ film ($\Delta d = 13 \pm 5$ nm), using the optical characterisation method mentioned in the text. The reported value for the thickness variation has been calculated by averaging the underlined Δds , as explained in the text

λ_{tan} (nm)	s	a_s	T_+	T_-	Δd (nm)	m	\bar{d} (nm)	n
1588	1.491	0.9831	0.903	0.623	22.3	3.5	1155	2.421
1395	1.495	0.9767	0.899	0.616	<u>14.5</u>	4.0	1150	2.430
1243	1.500	0.9737	0.896	0.611	<u>12.4</u>	4.5	1145	2.436
1124	1.498	0.9710	0.893	0.607	<u>11.3</u>	5.0	1147	2.448
1027	1.503	0.9726	0.892	0.605	<u>12.2</u>	5.5	1145	2.460
947	1.508	0.9754	0.893	0.604	<u>12.4</u>	6.0	1145	2.475
880	1.514	0.9799	0.895	0.603	<u>11.5</u>	6.5	1143	2.491
822	1.510	0.9842	0.898	0.604	<u>12.6</u>	7.0	1147	2.506
773	1.509	0.9875	0.900	0.604	<u>12.4</u>	7.5	1151	2.525
730	1.509	0.9909	0.900	0.602	<u>13.0</u>	8.0	1152	2.544
693	1.508	0.9932	0.898	0.598	<u>14.2</u>	8.5	1153	2.566
661	1.508	0.9951	0.892	0.589	<u>15.6</u>	9.0	1151	2.591
633	1.508	0.9968	0.868	0.575	20.2	9.5	1153	2.619
608	1.508	0.9980	0.821	0.544	24.2	10.0	1143	2.648
586	1.509	0.9992	0.716	0.496	28.0	10.5	1153	2.680
568	1.509	1.0000	0.584	0.420	26.3	11.0	1136	2.721
549	1.510	1.0000	0.405	0.305	20.0	11.5	–	2.750

4. Results

Transmission spectra corresponding to the as-deposited amorphous $\text{As}_{40}\text{S}_{60-x}\text{Se}_x$ films ($x = 0, 20, 30, 40$ and 60 at.%), prepared by thermal evaporation, are plotted in the inset of Fig. 1, showing a clear red shift of the interference-free region with increasing Se content. The results of the application of the above-described procedure for calculating the average thickness, the thickness variation and the refractive index, for a representative virgin amorphous $\text{As}_{40}\text{S}_{40}\text{Se}_{20}$ film, are listed in Table 1 for illustrative purposes. The optical transmission spectrum corresponding to this representative sample is displayed in Fig. 1, along with its upper and lower envelopes, which have been computer-drawn using the algorithm suggested by McClain et al. [19]. In addition, both the transmission and the reflection spectra of the uncoated substrate are also plotted in this figure. Absorption effects in the substrate are clearly evidenced from its transmission spectrum.

Alternatively, film thicknesses were directly measured by the mechanical profilometer. The measured value of the average thickness for the above-mentioned representative film was 1166 ± 18 (1.5%) nm, which is in excellent agreement with

the calculated value, 1148 ± 5 (0.4%) nm. Differences between mechanically measured and optically calculated average thicknesses of the films were, in all cases, less than 2%.

The dispersion of the refractive index has been analysed on the basis of the Wemple–DiDomenico (WDD) model [20,21], which is based on the single-oscillator formula

$$n^2(\hbar\omega) = 1 + \frac{E_o E_d}{E_o^2 - (\hbar\omega)^2}, \tag{5}$$

where E_o is the single-oscillator energy and E_d the dispersion energy or single-oscillator strength. E_o is considered as an ‘average’ energy gap and, to a good approximation, it varies in proportion to the Tauc gap, E_g^{opt} (which will be defined later, when the optical absorption edge is studied): $E_o \approx 2E_g^{\text{opt}}$ [22]. On the other hand, an important achievement of the WDD model is that it relates the dispersion energy, E_d , to other physical parameters of the material through the following empirical relationship [20,21]:

$$E_d = \beta N_c Z_a N_e \text{ (eV)}, \tag{6}$$

where N_c is the effective coordination number of the cation nearest neighbour to the anion, Z_a is the

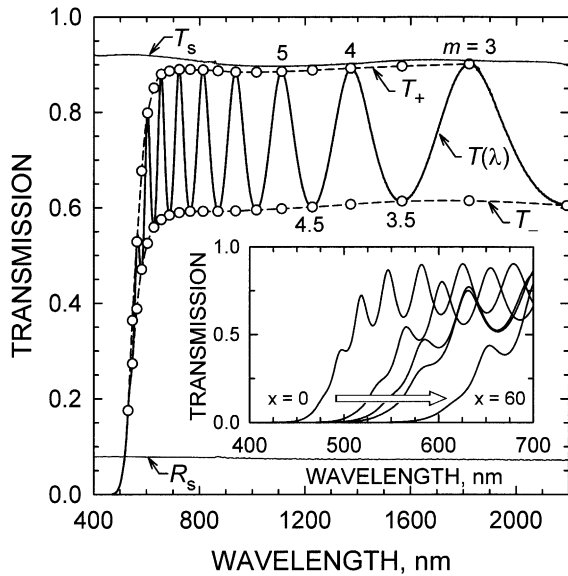


Fig. 1. Optical transmission spectrum, $T(\lambda)$, for a representative as-deposited thermally evaporated amorphous $\text{As}_{40}\text{S}_{40}\text{Se}_{20}$ film. The top, T_+ , and bottom, T_- , envelope curves are displayed, and the points at the wavelengths where those envelopes and the spectrum are tangential are marked. The transmission, $T_s(\lambda)$, and the reflection, $R_s(\lambda)$, spectra corresponding to the uncoated substrate are also plotted. The order numbers, m , for some tangential points are shown. The transmission spectra at short wavelengths for thermally evaporated amorphous $\text{As}_{40}\text{S}_{60-x}\text{Se}_x$ films ($x = 0, 20, 30, 40$ and 60 at.%) are plotted in the inset; a red shift of the interference-free region with increasing Se content can be seen.

formal chemical valency of the anion, N_e is the effective number of valence electrons per anion, and β is a two-valued constant with either an ionic or a covalent value ($\beta_i = 0.26 \pm 0.03$ eV and $\beta_c = 0.37 \pm 0.04$ eV, respectively).

By plotting $(n^2 - 1)^{-1}$ against $(\hbar\omega)^2$ and fitting a straight line, as shown in Fig. 2, E_o and E_d can be directly determined from the slope, $(E_o E_d)^{-1}$, and the intercept, E_o/E_d , on the vertical axis. Nevertheless, it must be noted that the WDD model is only valid in the transparent region, where the absorption coefficient of the chalcogenide film takes values $\alpha \approx 0$. Therefore, due to optical absorption, the experimental energy variation in the refractive index departs from that given by Eq. (5) when the photon energy approaches E_g^{opt} , as clearly shown in Fig. 2. The values of the parameters E_o

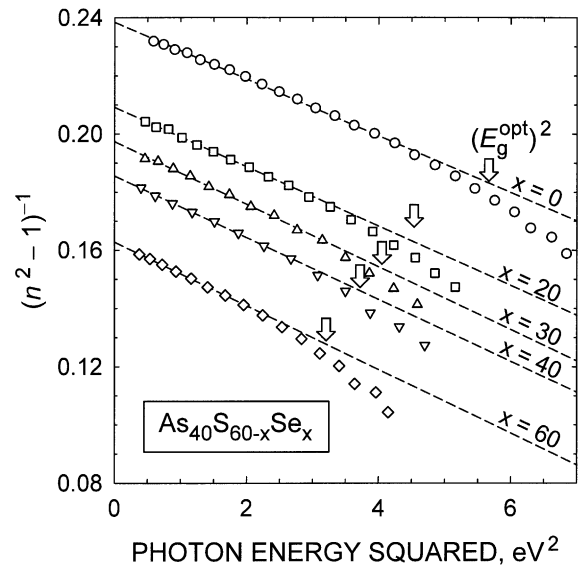


Fig. 2. Plot of the refractive-index factor $(n^2 - 1)^{-1}$ versus $(\hbar\omega)^2$, for as-deposited thermally evaporated amorphous $\text{As}_{40}\text{S}_{60-x}\text{Se}_x$ films. Dashed lines are the corresponding least-square linear fits. The values of the photon energy squared, corresponding to E_g^{opt} , are marked by vertical arrows.

and E_d , as well as the value of the refractive index at $\hbar\omega \rightarrow 0$ (extrapolating the WDD optical dispersion relationship towards the infrared spectral region), $n(0)$, for the as-evaporated amorphous $\text{As}_{40}\text{S}_{60-x}\text{Se}_x$ films ($x = 0, 20, 30, 40$ and 60 at.%), are all listed in Table 2. Furthermore, the compositional dependencies of E_o and E_d are both plotted in Fig. 3.

By extrapolating Eq. (5) towards shorter wavelengths, the refractive-index values can be estimated in the strong absorption region. Hence, either of the two equations collected in Eq. (3) can be solved to determine the values of the optical absorbance, a , in this spectral region and, subsequently, the values of the absorption coefficient, α . In particular, following Swanepoel's ideas [15,16], we have used the equation for the upper envelope, T_+ . The calculated optical absorption spectra, $\alpha(\hbar\omega)$, for the untreated amorphous $\text{As}_{40}\text{S}_{60-x}\text{Se}_x$ films under study, are displayed in Fig. 4, using a semi-logarithmic scale. A clear red shift of the absorption edge is observed with increasing Se content. Analysis of the high-absorption region

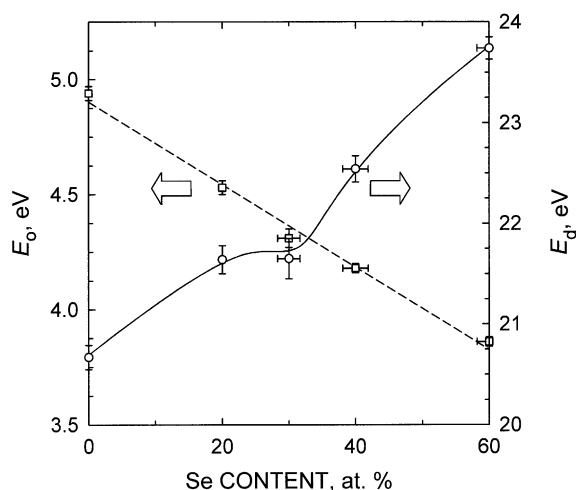


Fig. 3. Optical dispersion parameters, E_o and E_d , versus Se content. Solid and dashed lines are guides for the eye.

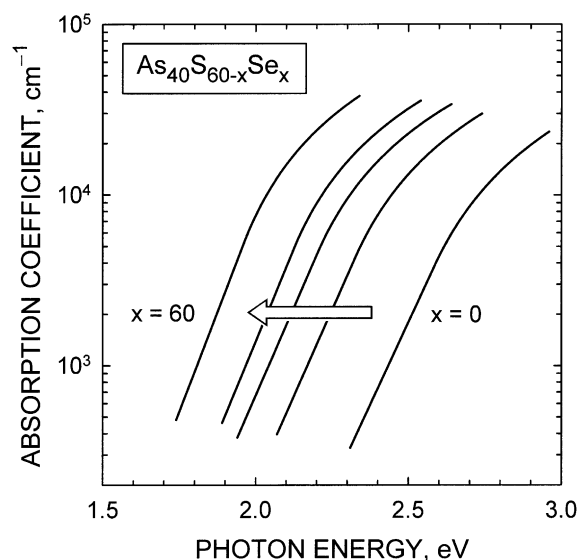


Fig. 4. Optical absorption spectra, $\alpha(\hbar\omega)$, for as-deposited thermally evaporated amorphous $As_{40}S_{60-x}Se_x$ films.

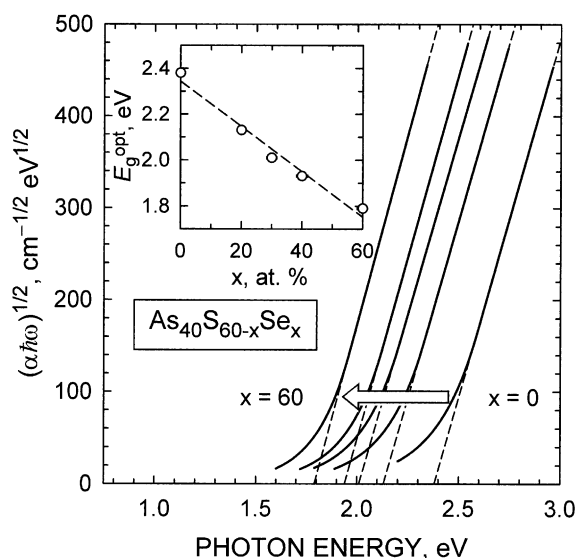


Fig. 5. Determination of the optical gaps in terms of Tauc's law, as linear extrapolation of the absorption data (dashed lines). The compositional dependence of E_g^{opt} is shown in the inset (the dashed line is a guide for the eye).

($\alpha \gg 10^4 \text{ cm}^{-1}$), has been carried out by the following quadratic equation, which is often called the Tauc law [23]:

$$\alpha(\hbar\omega) = B \frac{(\hbar\omega - E_g^{opt})^2}{\hbar\omega}, \quad (7)$$

where B is a constant, which depends on the electronic transition probability, and E_g^{opt} is the already introduced Tauc gap, now formally defined. The values of E_g^{opt} for the as-evaporated amorphous $As_{40}S_{60-x}Se_x$ films have been derived by plotting $(\alpha\hbar\omega)^{1/2}$ versus $\hbar\omega$ (see Fig. 5), and they are all listed in Table 2.

Table 2

Values of the optical dispersion parameters, E_o and E_d , refractive index for $\hbar\omega \rightarrow 0$, $n(0)$, As effective coordination number, N_c , and Tauc optical gap, E_g^{opt} , for the thermally evaporated amorphous $As_{40}S_{60-x}Se_x$ films under study

Se content (at.%)	E_o (eV)	E_d (eV)	$n(0)$	N_c	E_g^{opt} (eV)
0	4.94 ± 0.03	20.67 ± 0.12	2.277 ± 0.001	3.0 ± 0.3	2.38 ± 0.01
20	4.53 ± 0.03	21.64 ± 0.14	2.404 ± 0.001	3.1 ± 0.3	2.13 ± 0.01
30	4.31 ± 0.04	21.65 ± 0.20	2.454 ± 0.001	3.1 ± 0.3	2.01 ± 0.01
40	4.18 ± 0.02	22.54 ± 0.13	2.528 ± 0.001	3.2 ± 0.3	1.93 ± 0.01
60	3.86 ± 0.02	23.74 ± 0.11	2.674 ± 0.001	3.4 ± 0.3	1.79 ± 0.01

5. Discussion

Fig. 2 shows that the refractive index increases with increasing Se content, over the entire spectral range studied. This increase is related to the increased polarizability, α_p , of the larger Se atoms (atomic radius, 115 pm), in comparison with S atoms (atomic radius, 100 pm). It is well known [24] that the polarizability and the refractive index are linked by the Lorentz–Lorenz relationship

$$\frac{n^2 - 1}{n^2 + 2} = \frac{1}{3\epsilon_0} \sum_j N_j \alpha_{p,j}, \quad (8)$$

where ϵ_0 is the vacuum permittivity and N_j the number of polarizable units of type j per volume unit, with polarizability $\alpha_{p,j}$. The polarizability α_p that appears in Eq. (8), determining the refractive index, can have several physical origins. In particular, for covalent solids, in the optical spectral range, the electronic polarizability, which is associated with both the distortion of the electronic charge distribution in an atom relative to the ion core, and the distortion of the electronic charge density in covalent bonds, is dominant.

Eq. (8) can be expanded for the different contributions corresponding to the constituents of the alloys under study

$$\frac{n^2 - 1}{n^2 + 2} = \frac{1}{3\epsilon_0} [N_{As} \alpha_{p,As} + N_S \alpha_{p,S} + N_{Se} \alpha_{p,Se}]. \quad (9)$$

Taking into account the particular stoichiometry of the composition line, $As_{40}S_{60-x}Se_x$, Eq. (9) can be rewritten as follows:

$$\frac{n^2 - 1}{n^2 + 2} = \frac{1}{3\epsilon_0} \left[\left(\frac{2}{3} \alpha_{p,As} + \alpha_{p,S} \right) N + (\alpha_{p,Se} - \alpha_{p,S}) N_{Se} \right], \quad (10)$$

where $N = N_S + N_{Se}$ is a constant and $N_{As} = 2/3N$. According to Eq. (10), a linear dependence between the refractive-index factor $(n^2 - 1)/(n^2 + 2)$ and N_{Se} (or equivalently, x) should be expected. Plots of this factor as a function of Se content, for both our $n(0)$ values and the values of the refractive index at $\lambda = 5 \mu\text{m}$ reported by Sanghera et al. [7], for $As_{40}S_{60-x}Se_x$ bulk glasses, with $x = 0, 5, 10, 15$ and 20 at.%, are shown in Fig. 6. In both cases, the experimental data seem to be in very good

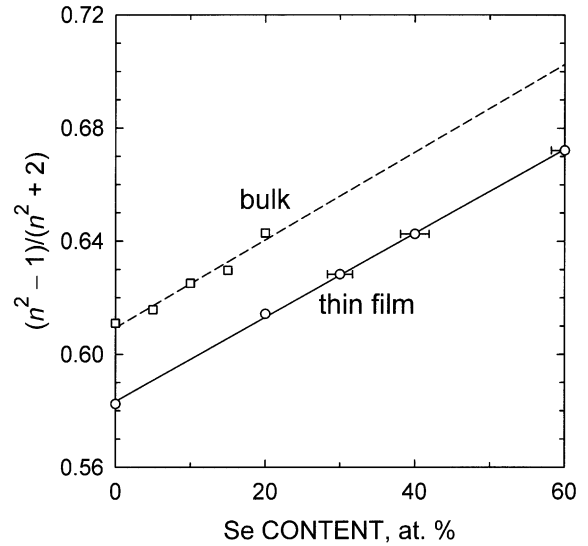


Fig. 6. Plots of the refractive-index factor $(n^2 - 1)/(n^2 + 2)$ as a function of Se content, according to the Lorentz–Lorenz relationship, for $\lambda \rightarrow \infty$ (or equivalently, $\hbar\omega \rightarrow 0$) and $\lambda = 5 \mu\text{m}$, for amorphous thin films and bulk glasses [7], respectively, with compositions along the $As_{40}S_{60-x}Se_x$ composition line.

agreement with the linear behaviour predicted by Eq. (10). We are assuming that $n(\lambda = 5 \mu\text{m}) \approx n(0)$, for the sake of comparison. The differences between the two plots shown in Fig. 6 could be explained on the basis of Eq. (8), taking into account the higher mass density of the bulk glasses in comparison with their thin-film counterparts [2,3]. Thus, the concentration of polarizable units, N_j , would be greater for bulk glasses than for as-evaporated films, leading to an increase of the values of the refractive index. The remarkable parallelism between both plots suggests that the structural differences between bulk glasses and as-evaporated amorphous chalcogenide films, which would introduce significant differences in the contribution to the electronic polarizability associated to the covalent bonds, seem not to be relevant for the values of the refractive index at the longer wavelengths considered, $n(0)$ and $n(\lambda = 5 \mu\text{m})$. Thus, the atomic contribution to the polarizability seems to be dominant for these particular refractive-index values.

It can be seen in Fig. 3 that the dispersion energy, E_d , increases with increasing Se content.

Taking into account Eq. (6), and assuming that the parameters $N_c = (40 \times 5 + 60 \times 6)/60 = 28/3$ and $Z_a = 2$ retain the same values along this particular composition line, it would seem reasonable to ascribe the trend observed in the values of E_d to an increase in the effective cation coordination number, N_c . On the other hand, the possible influence of the parameter β on the increase observed for the oscillator strength should be also mentioned. Thus, the nature of the chemical bonding could change towards being less ionic with increasing Se content. Nevertheless, according to Paulings' electronegativities, the ionicity of an As–S bond is $\approx 8\%$, while in the case of an As–Se bond it is $\approx 4\%$. Therefore, we will continue our discussion following the original WDD model, in which β is considered to be a constant, with the covalent value $\beta_c = 0.37 \pm 0.04$ eV.

It is well known [2] that the structure of binary As_2Ch_3 amorphous chalcogenides (Ch being a chalcogen atom) consists of locally two-dimensional structural layers, formed by AsCh_3 pyramidal units linked through a common twofold coordinated chalcogen atom, and interacting with each other by weak intermolecular bonds. Furthermore, it has been shown [5,6,10] that this picture is also valid for the structure of ternary $\text{As}_{40}\text{S}_{60-x}\text{Se}_x$ amorphous chalcogenides. In such cases, mixed $\text{AsS}_{3-n}\text{Se}_n$ ($n = 1$ or 2) pyramidal structural units have been reported [5,6,10] to be present in the amorphous matrix. According to Wemple [21], interactions between structural layers through As atoms acting as bonding points, forming $\text{As}\cdots\text{Ch}$ intermolecular bonds, would contribute to increase the As effective coordination number, and thus $N_c > 3$ is expected. In particular, for $\text{As}_{40}\text{S}_{60}$ bulk glass, Wemple suggests a value of $N_c \approx 3.2$. The values of N_c for as-evaporated amorphous $\text{As}_{40}\text{S}_{60-x}\text{Se}_x$ films derived from Eq. (6), are listed in Table 2.

Following Wemple's ideas [21], the overall increase observed in E_d (and consequently, in N_c) with increasing Se content, points towards a greater interaction between structural layers, which is consistent with the increase of the structural compactness for $\text{As}_{40}\text{S}_{60-x}\text{Se}_x$ bulk glasses, as reported by Sanghera et al. [7]. It is also important to mention that it has been very recently suggested

by Georgiev et al. [25] that fourfold coordinated As, in the form of quasi-tetrahedral $\text{Se} = \text{As}(\text{Se}_{1/2})_3$ units, in addition to the threefold coordinated As corresponding to the AsSe_3 pyramidal units, are building blocks of the Se-rich glasses, which also supports our higher-than-three As effective coordination-number results. Therefore, even though the inferred increase for N_c is almost within the error bars (see Table 2), we believe that the increase in E_d on which the above conclusion is based, is undoubtedly significant.

On the other hand, small deviations of the average molar volume, ΔV , from additivity of molar volumes of components, in bulk glasses in the system $(\text{As}_2\text{S}_3)_{1-y}(\text{As}_2\text{Se}_3)_y$, have been observed by Feltz [6] and Stronski et al. [26]. These deviations have been associated with a departure in the substitution of S by Se from the statistical case. Furthermore, quasi-spherical $\text{As}_4\text{S}(\text{Se})_4$, and S(Se) and As_4 molecular fragments have been reported to be embedded in both binary and ternary as-deposited $\text{As}_{40}\text{S}_{60-x}\text{Se}_x$ films, prepared by thermal evaporation [2–4]. These molecular clusters would make difficult the cohesion between the structural layers, and consequently, would also contribute to an increase of ΔV , as well as to a decrease of the As effective coordination number, N_c . This could explain the difference between the value of N_c found for our amorphous $\text{As}_{40}\text{S}_{60}$ films, $N_c \approx 3.0$, and the value inferred by Wemple [21] for the $\text{As}_{40}\text{S}_{60}$ bulk glass, $N_c \approx 3.2$. Therefore, the deviations from the statistical substitution of S by Se, as well as the presence of the above-mentioned molecular clusters in the amorphous matrix of the films, could both be related to the non-linear dependence of the dispersion energy, E_d , shown in Fig. 3. It should be emphasised that Vlcek et al. [10] have reported similar non-linear behaviour for the glass-transition temperature, T_g , relaxation enthalpy, ΔH , and specific heat capacity, C_p , for $\text{As}_{40}\text{S}_{60-x}\text{Se}_x$ bulk glasses, as well as for E_d in the case of well-annealed films of this particular glassy system.

The compositional dependence of E_g^{opt} is plotted in the inset of Fig. 5. A linear decrease in E_g^{opt} with increasing Se content has been found. A similar compositional dependence has been observed for the oscillator energy, E_o (see Fig. 3), as

expected according to the previously mentioned relationship due to Tanaka [22]. The higher bonding energy of As–S bonds ($379.5 \text{ kJ mol}^{-1}$) compared with that of As–Se bonds (96 kJ mol^{-1}), plausibly explains the decrease found in both optical parameters. It is interesting to point out that the molecular vapour species embedded in the as-evaporated amorphous $\text{As}_{40}\text{S}_{60-x}\text{Se}_x$ films ($\text{As}_4\text{S}(\text{Se})_4$, $\text{S}(\text{Se})$ and As_4), introduce homopolar bonds of the types As–As, S–S and Se–Se. Thus, even though the high-bonding energies of such homopolar bonds (382.0 , 425.3 and $332.6 \text{ kJ mol}^{-1}$, respectively) could somehow contribute to an increase of the value of both E_g^{opt} and E_o , according to our results they do not seem to play an important role in the behaviour of E_g^{opt} and E_o with changing x .

6. Conclusions

The optical properties of as-deposited amorphous $\text{As}_{40}\text{S}_{60-x}\text{Se}_x$ films ($x = 0, 20, 30, 40$ and 60 at.%), prepared by thermal evaporation, have been determined from their corresponding transmission spectra, measured at normal incidence. An improved envelope method to characterise non-uniform thin dielectric films optically and geometrically, which takes into account the weak absorption in the substrate, has been successfully employed, and it has allowed us to determine both the average thickness, \bar{d} , and the refractive index, n , of the films, with accuracies better than 1%. It has been found that the refractive index increases with increasing Se content over the entire spectral range studied. The analysis of the compositional dependence of the refractive index on the basis of the Lorentz–Lorenz equation suggests that this increase is related to the increased polarizability, α_p , of the larger Se atoms, in comparison with S atoms. It has been found that the dispersion parameter, E_d , increases non-linearly with increasing x , showing a plateau around $x = 30$ at.%. According to the model suggested by Wemple [21], it has been inferred that the increase of E_d points towards an increase in the interactions between the structural layers, hence leading to an increase of the As effective coordination number, N_c . Never-

theless, a decrease in the ionic character of the chemical bonding with increasing Se content, and its possible influence on the value of the parameter β , cannot be excluded either. The non-linear behaviour could be related to small deviations in the substitution of S by Se from the statistical case, as well as to the presence of molecular clusters embedded in the amorphous matrix of the as-evaporated $\text{As}_{40}\text{S}_{60-x}\text{Se}_x$ films. Finally, a linear decrease has been obtained in both E_o and E_g^{opt} , which is plausibly explained by taking into account the higher bonding energy of As–S bonds, in comparison with that of As–Se bonds.

Acknowledgements

The authors are grateful to Professor S.R. Elliott (Department of Chemistry, University of Cambridge, UK) for a critical reading of the paper. This work has been partly supported by a Marie Curie Fellowship of the European Community programme ‘Improving Human Research Potential and the Socio-Economic Knowledge Base’ under contract number HPMF-CT-2000-01031, and by the MCYT (Spain) and FEDER (CEE) under MAT2001-3333 project.

References

- [1] N.A. Goryunova, B.T. Kolomiets, Zh. Tekhn. Fiz. 25 (1955) 984.
- [2] S.R. Elliott, in: J. Zarzycki (Ed.), Materials Science and Technology, vol. 9, VCH, Weinheim, 1991, p. 375.
- [3] M.A. Popescu, Non-Crystalline Chalcogenides, Kluwer Academic, Dordrecht, 2000.
- [4] A.V. Kolobov, Ka. Tanaka, in: H.S. Nalwa (Ed.), Handbook of Advanced Electronic and Photonic Materials and Devices, vol. 5, Academic Press, San Diego, CA, 2001, p. 47.
- [5] J.A. Freitas, U. Strom, D.J. Treacy, J. Non-Cryst. Solids 59&60 (1983) 875.
- [6] A. Feltz, Amorphous and Inorganic Materials and Glasses, VCH, Weinheim, 1993.
- [7] J.S. Sanghera, V.W. Nguyen, I.D. Aggarwal, J. Am. Ceram. Soc. 79 (1996) 1324.
- [8] E. Márquez, J.M. González-Leal, R. Prieto-Alcón, M. Vlcek, A. Stronski, T. Wagner, D. Minkov, Appl. Phys. A 67 (1998) 371.

- [9] E. Márquez, J.M. González-Leal, R. Prieto-Alcón, R. Jiménez-Garay, M. Vlcek, *J. Phys. D* 32 (1999) 3128.
- [10] M. Vlcek, A.V. Stronski, A. Sklenar, T. Wagner, S.O. Kasap, *J. Non-Cryst. Solids* 266–269 (2000) 964.
- [11] A.V. Stronski, M. Vlcek, A. Sklenar, P.E. Shepeljavi, S.A. Kostyukevich, T. Wagner, *J. Non-Cryst. Solids* 266–269 (2000) 973.
- [12] E. Márquez, J.M. González-Leal, R. Jiménez-Garay, M. Vlcek, *Thin Solid Films* 396 (2001) 183.
- [13] J.S. Berkes, S.W. Ing Jr., W.J. Hillegas, *J. Appl. Phys.* 42 (1971) 4908.
- [14] J.C. Manifacier, J. Gasiot, J.P. Fillard, *J. Phys. E* 9 (1976) 1002.
- [15] R. Swanepoel, *J. Phys. E* 16 (1983) 1214.
- [16] R. Swanepoel, *J. Phys. E* 17 (1984) 896.
- [17] S.C. Chiao, B.G. Bovard, H.A. Macleod, *Appl. Opt.* 34 (1995) 7355.
- [18] J.M. González-Leal, R. Prieto-Alcón, J.A. Angel, D.A. Minkov, E. Márquez, *Appl. Opt.* (submitted 18 February 2002).
- [19] M. McClain, A. Feldman, D. Kahaner, X. Ying, *Comput. Phys.* 5 (1991) 45.
- [20] S.H. Wemple, M. DiDomenico, *Phys. Rev. B* 3 (1971) 1338.
- [21] S.H. Wemple, *Phys. Rev. B* 7 (1973) 3767.
- [22] Ke. Tanaka, *Thin Solid Films* 66 (1980) 271.
- [23] J. Tauc, in: J. Tauc (Ed.), *Amorphous and Liquid Semiconductors*, Plenum, New York, 1974, p. 159.
- [24] S.R. Elliott, *The Physics and Chemistry of Solids*, Wiley, Chichester, 2000.
- [25] D.G. Georgiev, P. Boolchand, M. Micoulaut, *Phys. Rev. B* 62 (2000) R9228.
- [26] A.V. Stronski, M. Vlcek, P.F. Oleksenko, *Semicond. Phys., Quantum Electron. Optoelectron.* 4 (2001) 210.